JMEPEG (2020) 29:6033–6043
https://doi.org/10.1007/s11665-020-05082-4

1059-9495/$19.00

Assessment of Cooling Performance of Neem Oil for Distortion Control in Heat Treatment of Steel

K.M. Pranesh Rao and K. Narayan Prabhu

(Submitted March 28, 2020; in revised form July 20, 2020; published online September 9, 2020)

Growing concerns over the hazardous impact of mineral oil-based industrial quench media on human health and the environment have forced researchers to seek renewable and non-hazardous alternatives. Non-edible vegetable oil-based quench media are perceived to be a potential replacement for mineral-based industrial quench media. The present work focuses on assessing the cooling performance of neem oil as compared to commercial hot oil quench media. Inconel and steel probes were used to characterize the cooling performance of these quench media maintained at bath temperatures 100 °C, 150 °C and 200 °C. The heat extraction rates and uniformity of heat extraction in Inconel probes quenched in neem oil were observed to be substantially higher at all bath temperatures. The hardness of AISI 52100 steel probe quenched in neem oil at all bath temperatures was observed to be higher. The pearlitic microstructure was observed in the steel probe quenched in hot oil maintained at 200 °C bath temperature. In contrast to this, a mixture of bainite, martensite and carbide was observed in case of steel probes quenched in neem oil maintained at 200 °C. Oxidation experiments revealed that neem oil is susceptible to an increase in viscosity due to oxidation. An increase in the viscosity by about 15% was observed in the case of neem oil as compared to only 4% increase in viscosity of hot oil. However, after an initial increase, the viscosity of neem oil stabilized and further no significant change in viscosity due to oxidation were observed. Oxidation had no significant effect on the cooling performance hot neem oil quench medium, and thus, it can be considered as an effective replacement for hot oil.

Keywords bio quenchants, heat treatment, inverse heat transfer, oxidation, steel

1. Introduction

Oil quench media are the most common quenchants used in the heat-treating industry (Ref 1). Mineral oil possesses several environmental problems and fire risks; nevertheless, 85% of heat-treating industries use these quench media (Ref 2). The petroleum-based quench oils can be broadly classified into four types, namely normal-speed quench oils, medium-speed quench oils, high-speed quench oils and marquenching oils or hot oils (Ref 3). Normal-, medium- and high-speed oils are used to quench harden steel parts of different grades and section sizes. The operating temperature does not exceed 50 °C. These oils contain paraffinic and naphthenic fractions. Antioxidants, accelerators and emulsifiers are added to the base oil to improve the service life of the oil, enhance cooling performance and ease post quench cleaning of steel parts, respectively (Ref 4).

Martempering oils are formulated from refined paraffinic base oils with high thermal stability. Carefully selected and tested antioxidants are added to retard the aging process. The kinetics of oxidation reaction doubles with ever 10 °C increase in operating temperature (Ref 5). The operating temperature for martempering oil ranges between 100 and 200 °C. Thermal aging and oxidation are thus the main factors considered during the selection of martempering oils.

Vegetable oil-based quench media are perceived to be a suitable replacement for non-renewable mineral oil-based quench oil. Unlike mineral oils, vegetable oils are biodegradable and non-toxic. Vegetable oils are a mixture of various triglycerides of fatty acids. Based on the number of carbon–carbon double bonds in the fatty acid, ester structural components of the different vegetable oil triglycerides are broadly classified into three types, (1) saturated, (2) monounsaturated and (3) polyunsaturated fatty acids.

Mineral oil and vegetable oils undergo oxidation in three stages, namely initiation, propagation and termination. The oxidation products in mineral oil form high molecular weight oligomers which settle as sludge in the quench tanks and increase the viscosity of the oil (Ref 6).

Vegetable oils have a limitation of relatively poor oxidative stability properties. The strength of a carbon–hydrogen bond next to a carbon–carbon double bond is lower, and this hydrogen can be removed easily during the oxidation reaction. Thus, carbon–carbon double bonds function as active sites for the oxidation reaction. In other words, the oxidation stability of vegetable oil decreases with an increase in unsaturated fatty acid content. During the termination of vegetable oil oxidation, hydroperoxides decompose to form numerous volatile and non-volatile secondary oxidation compounds. Hydroperoxides undergo polymerization reactions leading to deposits and an increase in viscosity of the oil (Ref 7). The effect of oxidation results in greater variation in the quench performance of vegetable oils compared to that observed in conventional petroleum oil quenchants (Ref 8).

K.M. Pranesh Rao and **K. Narayan Prabhu**, Department of Metallurgical and Materials Engineering, National Institute of Technology Karnataka, Surathkal, Srinivasnagar, Mangalore 575 025, India. Contact e-mails: praneshraokm@gmail.com and prabhukn_2002@yahoo.co.in.

Totten et al. (Ref 9) compared quench cooling performance of commercial mineral quench with crude expelled soya bean oil and partially winterized and hydrogenated soybean oil. The quench cooling characteristics of these vegetable oils were better than that of the mineral oil. Pranesh and Prabhu (Ref 10) studied quench performance of olive oil, rice bran oil and canola oil and some mineral oil blends. A very short duration of vapor blanket stage was observed in these vegetable oils which resulted in faster heat extraction rates compared to mineral oil.

Grossman's H factor for sunflower oil, coconut oil and palm oil is higher than mineral oil, this indicates better quench performance offered by the above vegetable oils. However, groundnut oil and castor oil have lower Grossman H factor compared to mineral oil (Ref 11).

The use of edible vegetable oils for heat treatment will cause a shortage of oils in the food processing industry. Non-edible vegetable oils are therefore preferable as quenching media. Vignesh and Prabhu assessed quench performance of non-edible vegetable oils, namely neem (*Azadirachta indica*) oil and Karanja (*Pongamia pinnata*) oil (Ref 12). They concluded that these non-edible vegetable oils are potential quench media to heat treat the steel. Hassan. et al. observed that neem oil can be used where cooling severity less than that of water, but greater than SAE 40 engine oil is required for hardening of plain carbon steels and ductile cast iron (Ref 13).

The inverse heat transfer method is widely used to experimentally calculate the quench heat flux and heat transfer coefficient. Kim et al. (Ref 14) showed that the heat transfer coefficient obtained by the inverse method is accurate and can be used to simulate the heat treatment process. Nie et al. (Ref 15) used experimentally determined heat transfer coefficients to simulate hardness and distortion in a medium-precision steel component with quenched in water and UCON (an aqueous polymer quench medium).

The present work explores the possibility of using neem oil for high-temperature quenching applications. The performance of neem oil quench media was compared with mineral oil-based martempering/hot oil maintained at elevated bath temperature. The study of the effect of oxidation on the viscosity of neem oil was also conducted.

2. Experimental Details

Figure 1 illustrates the sequence of experiments performed in this work. Figure 2 shows the experimental setup used for quench media characterization experiments. 1-mm- and 1.5-mm-diameter K-type thermocouples were inserted into the holes in Inconel and steel probes, respectively. The design of Inconel and steel probes is shown in Fig. 1(b) and (c), respectively. Inconel and steel probes have the same geometry but a different number of holes and hole diameters. 1-mm holes in the Inconel probe were EDM-drilled, and 1.5-mm holes in steel probes were drilled using a conventional drilling machine. The same Inconel probe was used for all quenching experiments, whereas separate steel probes were used for each experiment. The changes in the number of thermocouple holes and its dimensions in the steel probes are considering the economic viability of the experiments. The thermocouples inserted in the holes facilitate acquiring time–temperature data at the respective locations. The thermocouples were inserted into the probe through a 750-mm-long stainless-steel tube of 16 mm internal diameter. The lower end of the tube was fastened to the 5-mm-length M16 thread at the top end of the instrumented probe. The thermocouples were connected to the data acquisition system (NI-Daq9213) via compensating cables. The temperature data were acquired in the PC at a rate of 10 readings per second.

Hot oil and neem oil were the quench media selected for quenching experiments. Stainless steel container containing 2 L of quench media was heated in a quench bath furnace and maintained at the required bath temperature. The cooling performance of these media was assessed at a bath temperature of 100 °C, 150 °C and 200 °C.

The probe–tube–thermocouple arrangement was heated in the furnace to 860 °C. In the case of steel probes, the probe was maintained at 860 °C for 20 min for austenitizing. Following this, the probe was lowered into the quench media placed below the heating furnace. The guide was used to ensure straight and seamless manual lowering of probe–tube–thermocouple arrangement into the quench media. Pins were used to arresting the positions during heating and quenching of probe. For steel probe quenching experiments, the probe was held in the quench media until the temperature at the geometric center of the probe was 50 °C above bath temperature. Following this, the probe was removed from quench media and subjected to air cooling to room temperature.

The quenched-air cooled steel probes were cut at a depth of 35 mm and subjected to metallographic polishing. The polished steel samples were etched with 10% potassium metabisulfite.

The 30 ml of hot oil and neem oil was measured in open glass beakers and subjected to oxidation in a hot air oven. Six samples of each neem and hot oil were subjected to oxidation. The temperature of oil was maintained at 120 °C over the entire period of the experiment. One beaker containing oil sample was taken out after a duration of 8, 16, 24, 32, 40 and 48 h. Brookefield DV-III ultra-programmable rheometer was used to measure the viscosity of these samples. The viscosity was measured at a temperature of 40 °C.

3. Results and Discussion

3.1 Quenching of Inconel Probe

Figure 3 shows the cooling curves acquired at various locations in the Inconel probe quenched in hot and neem oil quench media maintained at different bath temperatures. The cooling curve data were used as an input to calculate the spatiotemporal quench heat flux. Y_1, Y_2, Y_3 and Y_4 are the temperatures sensed by the thermocouples inserted into the Inconel probe at a radial distance of 4.25 mm and depths of 12.5 mm, 27.5 mm, 42.5 mm and 57.5 mm from the top end of the probe, respectively. Y_c is the temperature measured at the geometric center of the Inconel probe.

The inverse heat transfer method was used to calculate the spatiotemporal heat flux. The quench heat flux was defined as a cubic function of distance as shown in Eq. 1. The mathematical and computational aspects of calculating time-dependent parameters p_1, p_2, p_3 and p_4 have been discussed in (Ref 16). Figure 4 shows spatiotemporal variation of quench heat flux during quenching of Inconel probe in hot and neem oil quench media maintained at different quench bath temperatures .The calculated heat flux was observed to vary significantly with

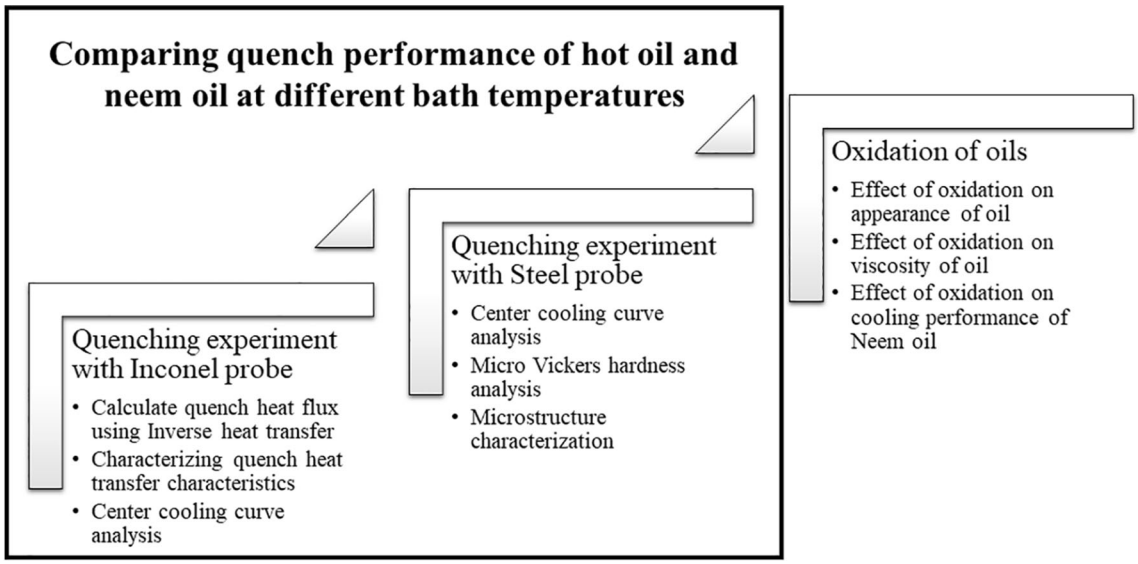

Fig. 1 Sequence of experiments

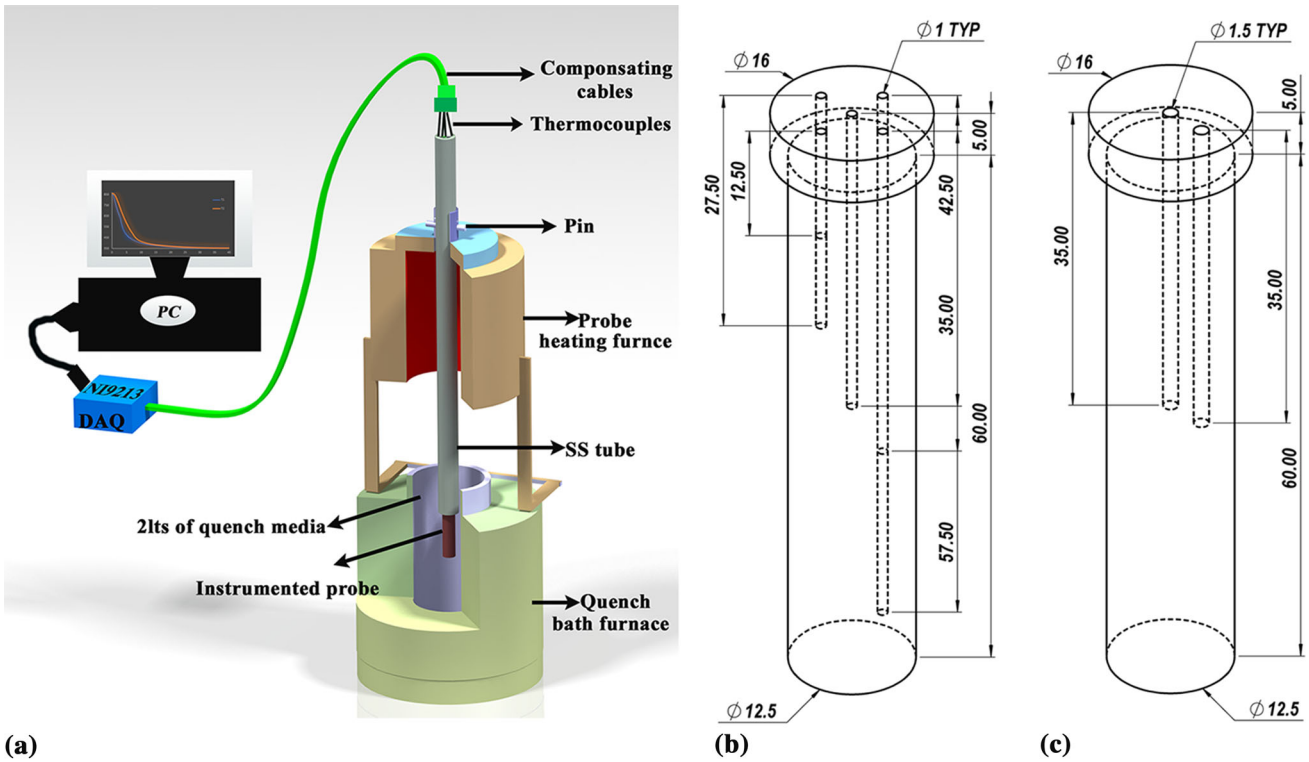

Fig. 2 (a) Experimental setup, (b) Inconel quench probe, (c) AISI 52100 steel probe

spatial location z. z is the distance measured from the bottom of the probe. The thermophysical properties of the Inconel probe were taken from (Ref 17).

$$q(t,z) = p_1(t)\,z^3 + p_2(t)\,z^2 + p_3(t)\,z + p_4(t) \qquad \text{(Eq 1)}$$

The heat flux was calculated using the temperature data obtained from thermocouples placed at locations 2 mm from the surface of the probe. The data from the thermocouple placed at the geometric center (T_C) were not used for inverse calculations. Figure 5 shows the transient variation of %Error between calculated and measured temperatures. %Error provides a fair insight into the accuracy of the calculated quench heat flux. The maximum %Error was observed to be in the range of ± 8%.

As shown in Fig. 6, the rate of increase in the mean heat flux in the initial stage of quenching in hot mineral oil was not as swift as that observed in neem oil. This suggests presence of an unstable vapor blanket stage. The vapor blanket stage was also observed in neem oil maintained at 200 °C bath temperature. In the case of hot oil and neem oil at 200 °C, heat flux increased to a peak value during the nucleate boiling stage after vapor blanket stage. Further, the heat flux decreased with temperature

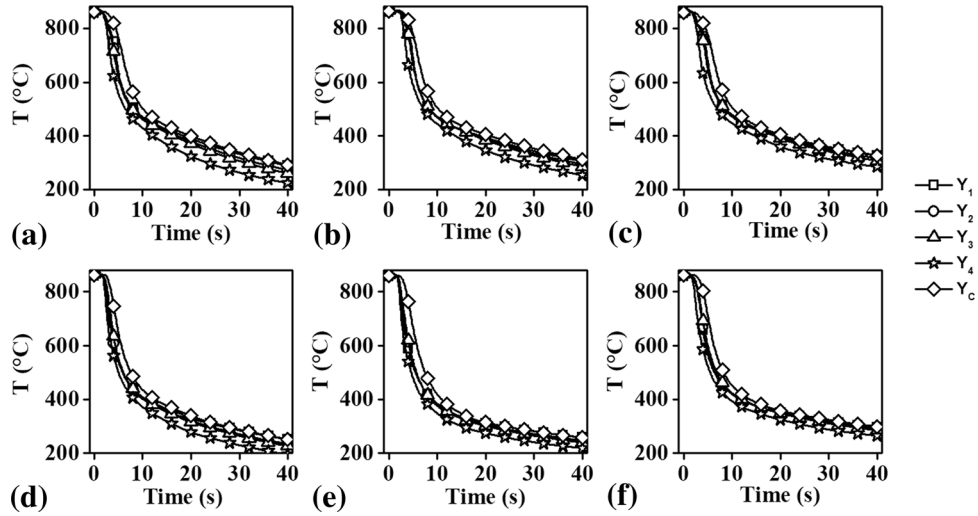

Fig. 3 Temperature measured in the Inconel probe cooling in hot oil maintained at (a) 100 °C, (b) 150 °C, (d) 200 °C and neem oil maintained at (c) 100 °C, (e) 150 °C, (f) 200 °C

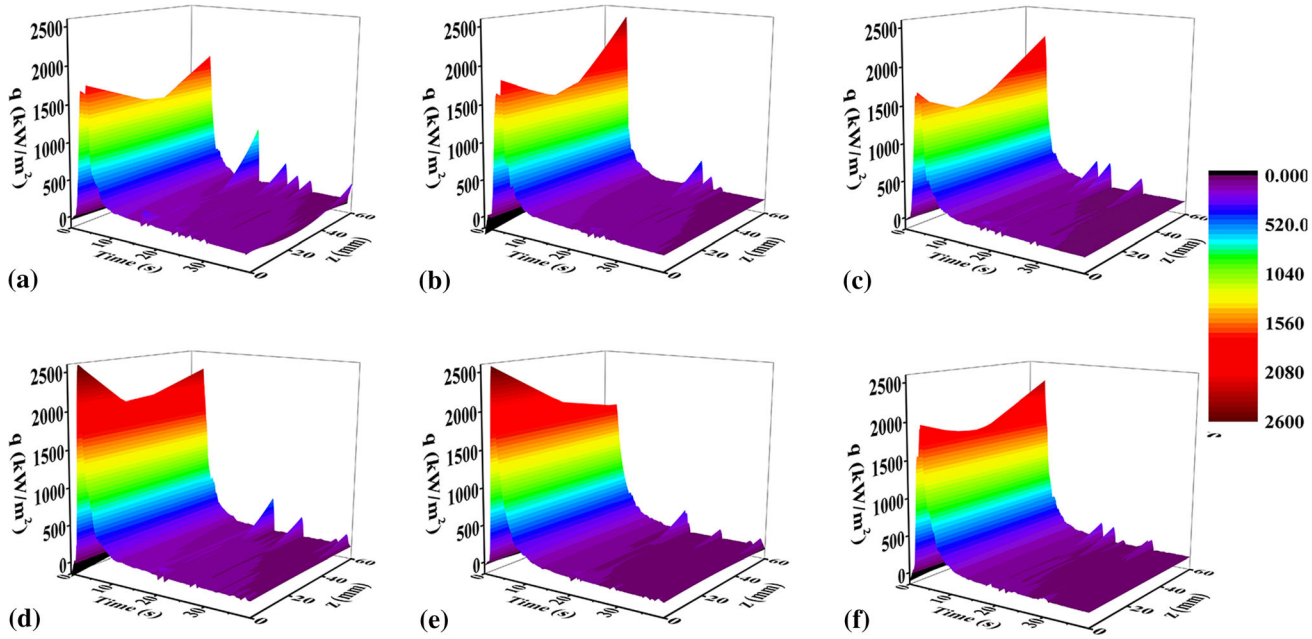

Fig. 4 Spatiotemporal variation of quench heat flux calculated for Inconel probe cooling in hot oil maintained at (a) 100 °C, (b) 150 °C, (c) 200 °C and neem oil maintained at (d) 100 °C, (e) 150 °C, (f) 200 °C

and the convective cooling stage started at lower temperatures (< 500 °C). As opposed to the conventional three-stage cooling observed during quenching in hot oil, heat transfer during quenching in neem oil maintained at 100 and 150 °C occurred in two stages, namely boiling and convective cooling stage.

Figure 7 shows the spatial variation of quench heat energy at the metal quenchant interface extracted in the first 40 s of quenching. The values were obtained by integrating spatially dependent heat flux over time as shown in Eq. 2. Higher energy was extracted from the bottom portion of the probe compared to that from the top portion of the probe. However, the variation in hot oil was much higher compared to hot oil.

Table 1 shows the quench heat flux parameters for hot oil and neem oil maintained at various quench bath temperatures. In Table 1, q_{max} is peak mean heat flux and T_{max} is corresponding mean surface temperature. T_{conv} and q_{conv} are mean temperature and mean peak heat flux corresponding to the start of the convective cooling stage. U is uniformity parameter, calculated using Eq. 3. Uniformity parameter quantifies the variation of quench heat energy extracted along the Inconel probe surface about average heat energy extracted ($\bar{E}_z$). The lower value of uniformity parameter represents more uniform cooling.

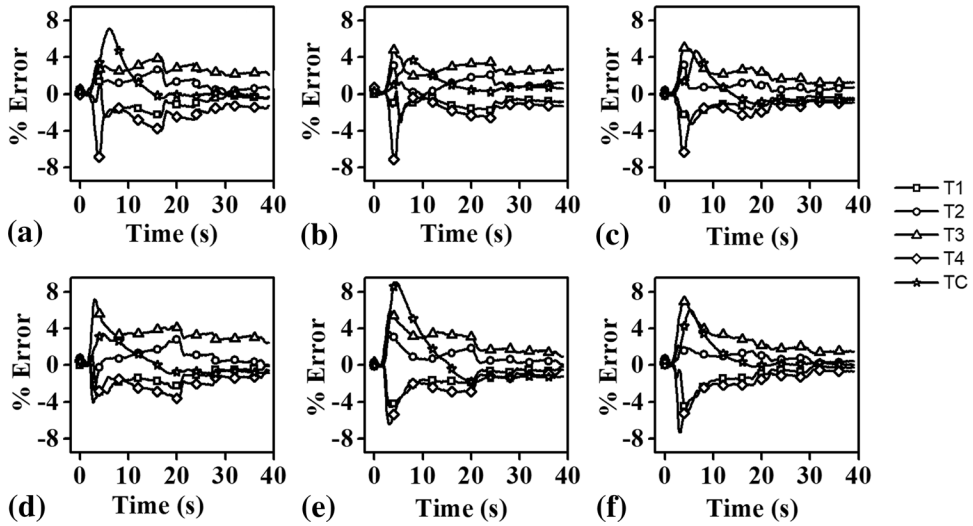

Fig. 5 Percentage error between measured and estimated temperatures in Inconel probe cooling in hot oil maintained at (a) 100 °C, (b) 150 °C, (c) 200 °C and neem oil maintained at (d) 100 °C, (e) 150 °C, (f) 200 °C

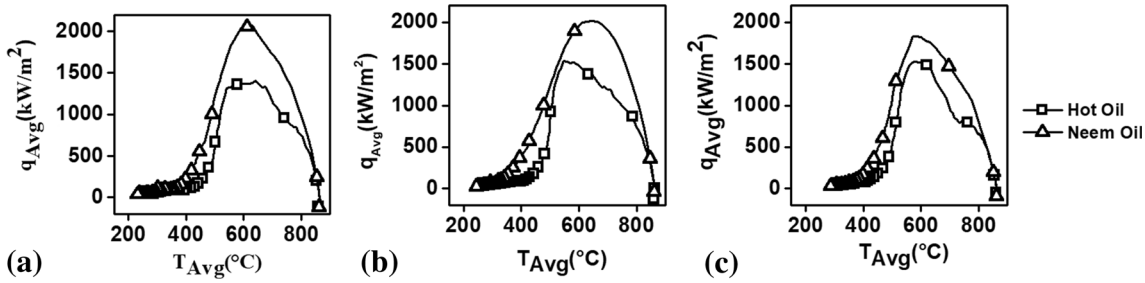

Fig. 6 Mean heat flux vs. mean surface temperature during cooling of Inconel probe in hot oil and neem oil maintained at (a) 100 °C, (b) 150 °C, (c) 200 °C

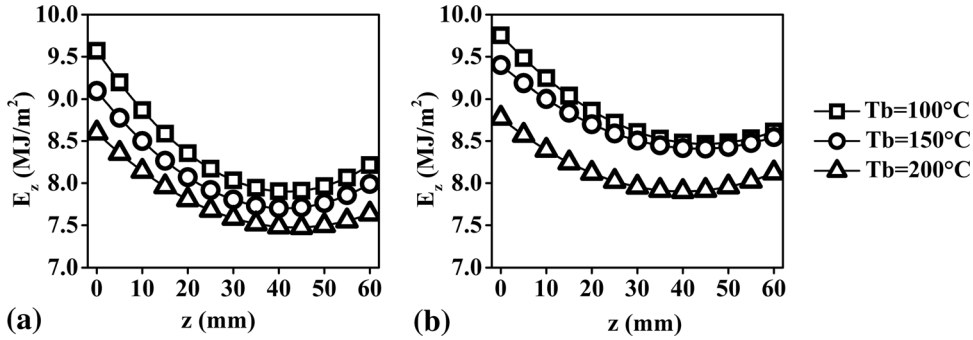

Fig. 7 Spatial variation of heat energy for Inconel probe quenched in (a) hot oil, (b) neem oil maintained at different bath temperatures

$$E_z(z) = \int_0^t q(z,t)\mathrm{d}z \quad t = 40\,\mathrm{s} \qquad \text{(Eq 2)}$$

$$\bar{E}_z = \frac{1}{l}\int_0^l E_z(z)\mathrm{d}z \quad l = 60\,\mathrm{mm} \qquad \text{(Eq 3)}$$

$$U = \frac{1}{l}\sqrt{\left(\int_0^l (E_z(z) - \bar{E}_z)^2\mathrm{d}z\right)} \quad l = 60\,\mathrm{mm} \qquad \text{(Eq 4)}$$

The values of q_{conv} and $q_{\max}$ in neem oil were higher than hot oil. Higher values of $q_{\max}$ and values of $T_{\max}$ near pearlite nose of steel are conducive to avert high-temperature diffusion-

Table 1 Mean quench heat flux parameters

Medium	T_b, °C	q_{max}, kW/m^2	T_{max}, °C	q_{Conv}, kW/m^2	T_{conv}, °C	U, kJ/m^2
Hot oil	100	1404	640	220	458	60
	150	1535	547	225	454	50
	200	1532	581	204	461	41
Neem oil	100	2072	629	293	412	48
	150	2014	645	239	369	36
	200	1832	585	267	420	31

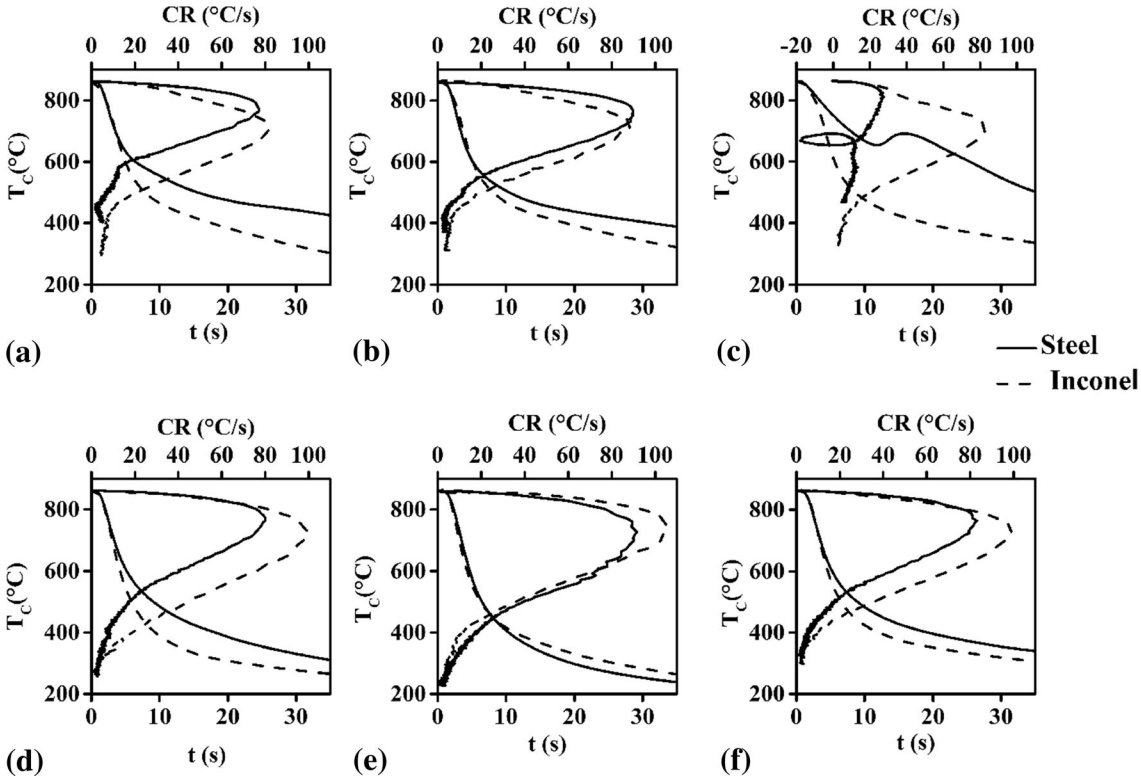

Fig. 8 Cooling and rate curves obtained at the geometric center of Inconel and AISI-52100 quenched in hot oil maintained at (a) 100 °C, (b) 150 °C, (c) 200 °C and neem oil maintained at (d) 100 °C, (e) 150 °C, (f) 200 °C

based transformation of austenite to ferrite, pearlite and cementite. No significant difference in the values of T_{conv} was observed in the case of hot oils. T_{conv} values for hot oil were significantly higher compared to that for neem oil. The start of the convective cooling stage at higher surface temperature would result in the slow cooling of steel specimens in the bainitic and martensitic transformation range. The slow cooling in the bainitic transformation range results in the transformation of austenite to the upper bainite phase; this phase reduces the overall hardness of the steel.

The uniformity parameter decreased with bath temperature in hot oil and neem oil. The degree of uniform cooling thus decreased with bath temperature in both quench media. For a given bath temperature, the Inconel probe quenched in neem oil was cooled with more uniformity as compared to hot oil. From Table 1 it can be concluded that neem oil offered higher cooling rates with increased uniformity of cooling as compared to the hot oil at all bath temperatures.

3.2 Quenching of Steel Probes

Figure 8 shows the cooling and rate curves for Inconel and AISI-52100 steel probes measured at the geometric center of the probe. The difference in cooling profiles of Inconel and steel probes is due to the difference in thermophysical properties and evolution of latent heat of transformation associated with the transformation of austenite in the course of cooling of steel probe. The vapor blanket stage was not observed during the quenching of steel probes in hot oils maintained at 100 and 150 °C.

A significant effect of latent heat of transformation was observed in steel probe quenched in hot oil maintained at 200 °C. The latent heat of transformation of austenite to pearlite and cementite in the probe resulted in the increase in temperature at the geometric center of the probe. This resulted in the loop observed in the cooling rate curve as observed in Fig. 8(c).

Figure 9(b) shows the variation of the measured hardness of AISI-52100 steel probes with bath temperature. Irrespective of bath temperature, higher hardness values were observed in neem oil as compared to hot oil. TTT diagram shown in Fig. 9(a) was generated using JMatPro software. Steel probe quenched in neem oil maintained at 200 °C and in hot oil maintained at 150 °C was observed to have higher hardness as compared to other bath temperatures in the respective quench media.

Figure 10, 11 and 12 shows the micrographs for AISI-52100 steels quenched in hot oil and neem oil maintained at 100 °C, 150 °C and 200 °C, respectively. Unresolved martensite, resolved martensite, carbides and upper bainite were observed in the microstructure of steel probe quenched in hot oil maintained at 100 °C. Resolved martensite refers to plate martensite with needle like structure. At this magnification, it is very difficult to determine the type of martensite present in unresolved martensite. It is most likely that the structure is a

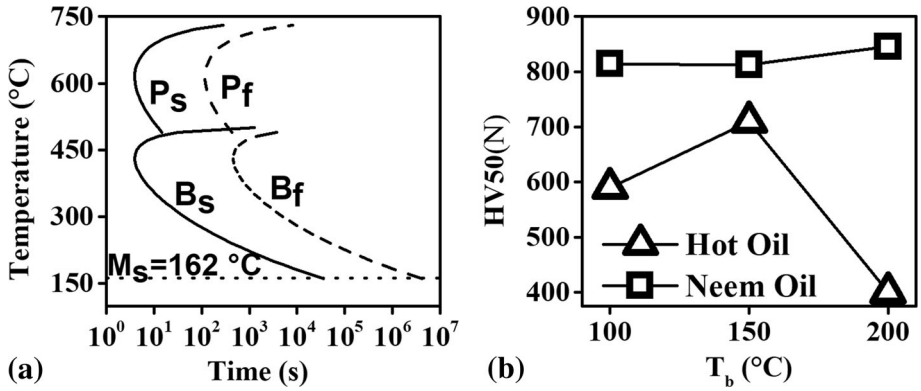

Fig. 9 (a) TTT diagram for AISI-52100 steel and (b) variation of average measured in steel probe quenched in hot oil and neem oil

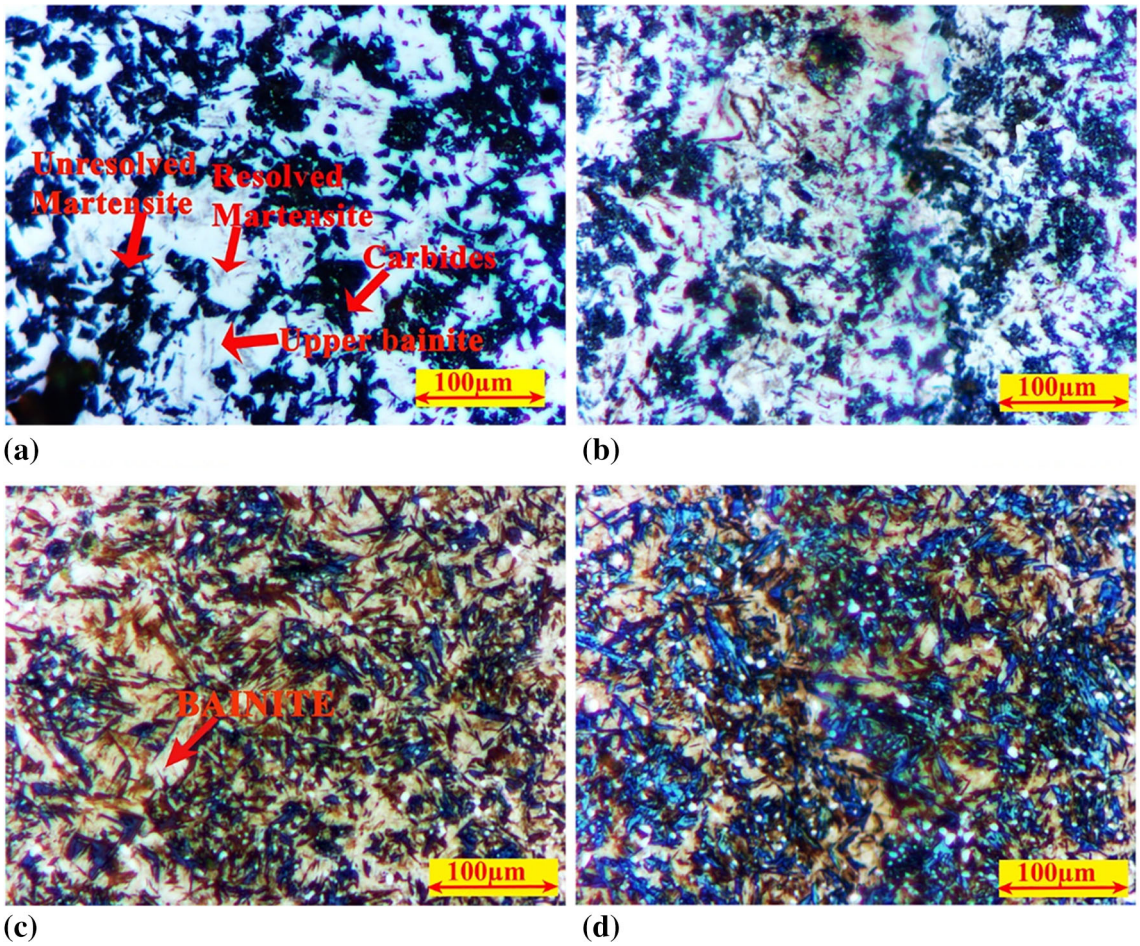

Fig. 10 Micrographs of AISI-52100 probe quenched in hot oil at (a) center, (b) near surface and neem oil at (a) center, (b) near surface for bath temperature of 100 °C

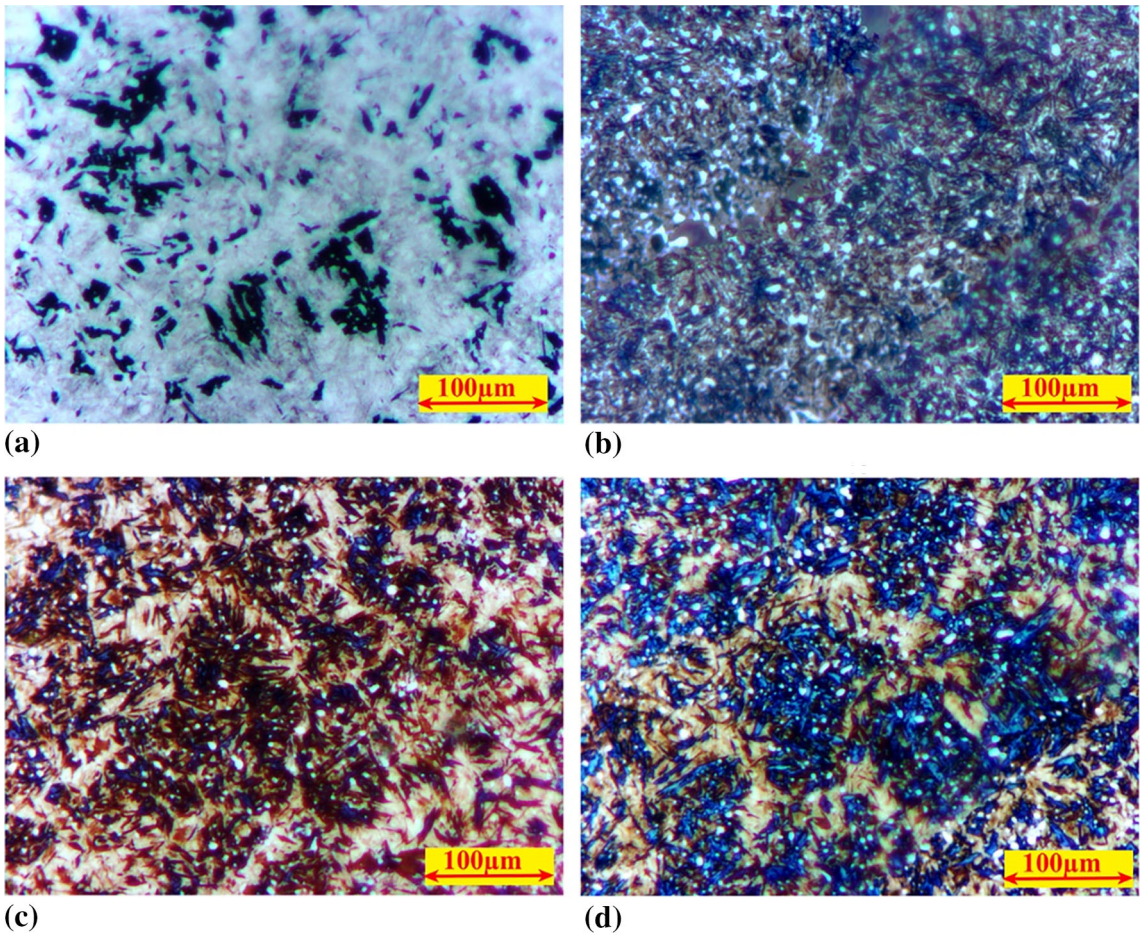

Fig. 11 Micrographs of AISI-52100 probe quenched in hot oil at (a) center, (b) near surface and neem oil at (a) center, (b) near surface for bath temperature of 150 °C

complex mixture of lath and plate martensites. From the cooling curves for steel probe quenched in hot oil maintained at 100 °C, a significant drop in the cooling rate was observed below 600 °C. This region corresponds to the pearlite nose in the TTT diagram. The latent heat of transformation of austenite to carbide and upper bainite was the reason for the decrease in the cooling rate. The volume fraction of martensite was higher at the surface of this steel specimen. A mixture of martensite, bainite and small grains of carbides was observed in steel samples quenched in neem oil maintained at 100 °C.

The volume fraction of unresolved martensite observed at the center of the steel sample quenched in hot oil maintained at 150 °C was higher than that observed in steel sample quenched in hot oil maintained at 100 °C bath temperature. A mixture of lower bainite, small carbide and martensite was observed near the surface of these samples. The microstructure in steel samples quenched in neem oil maintained at 150 °C was similar to that observed in steel samples quenched in neem oil maintained at 100 °C.

In steel samples quenched in hot oil maintained at 200 °C bath temperature, a mixture of pearlite and cementite phase was observed. In the case of samples quenched in neem oil maintained at 200 °C, a mixture of bainite, martensite and large carbide was observed. The increase in hardness is due to the evolution of large carbides observed in the microstructure. This transformation is not desired during hardening heat treatment.

3.3 Oxidation of Oils

Figure 13 shows the change in the appearance of the oil due to oxidation. Both oils were observed to evolve darker with the progress of oxidation.

Fluid viscosity is the thermophysical property with the greatest effect on heat transfer during quenching (Ref 18). Figure 14 shows the effect of oxidation on the viscosity of hot oil and neem oil. No significant effect of oxidation was observed on the viscosity of hot oil. A marginal change of 4% was observed. In neem oil, the viscosity increased by 15% after 24 h of oxidation. No significant increase in viscosity was observed for the next 24 h. The viscosity of the neem oil sample thus stabilized after initial oxidation

The effect of oxidation of neem oil on the cooling performance was also assessed. Figure 15 compares the temperature-dependent cooling rate curve at the geometric center of the Inconel probe quenched in non-oxidized and oxidized neem oil maintained at 150 °C. The neem oil was oxidized by subjecting it to multiple cycles of quenching and maintaining bath temperature in the range of 100-200 °C. The viscosity of the oxidized neem oil was 0.465 Pa s. The viscosity was $\sim$ 10% higher as compared to the viscosity of non-oxidized neem oil which was 0.43 Pa s at 40 °C.

Figure 15 shows the cooling rate plotted as a function of temperature measured at the geometric center of the Inconel probe quenched in oxidized and non-oxidized neem oil quench

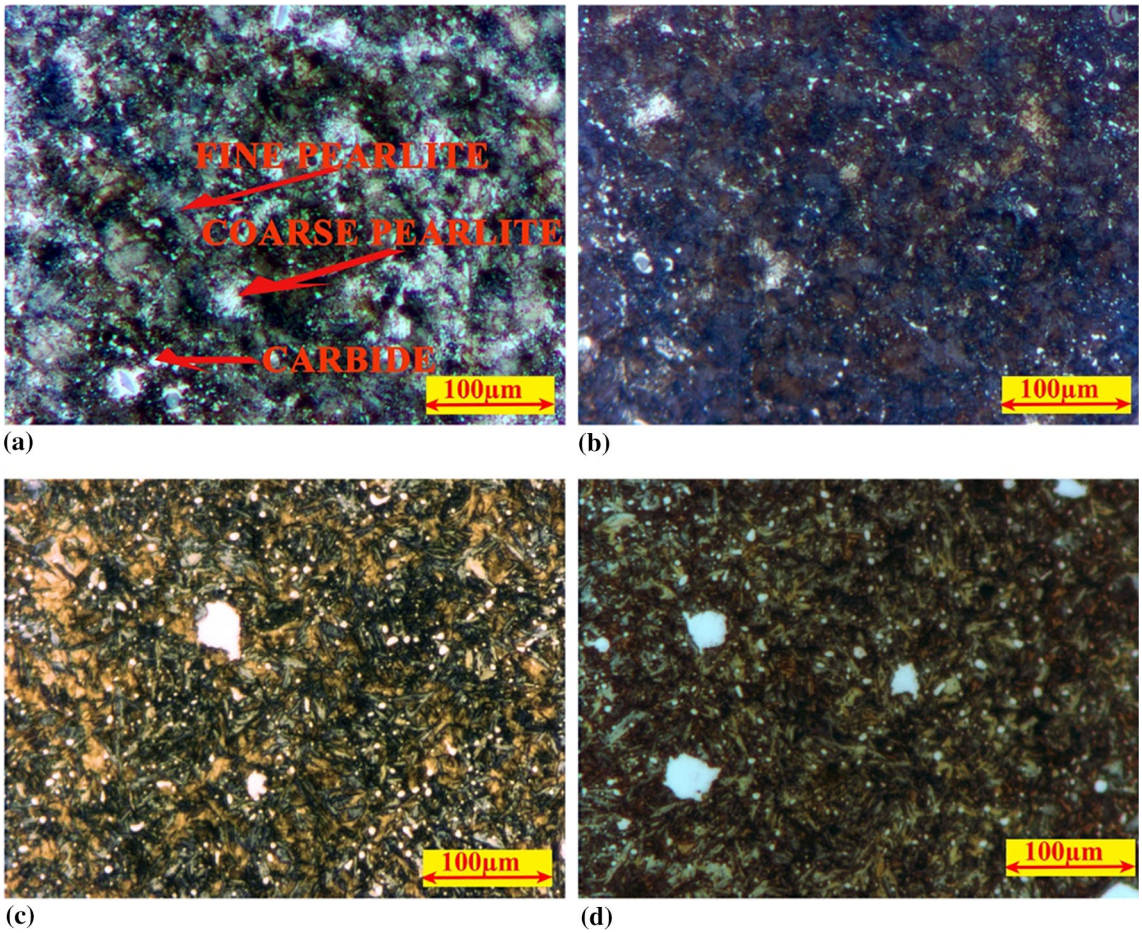

Fig. 12 Micrographs of AISI-52100 probe quenched in hot oil at (a) center, (b) near surface and neem oil at (a) center, (b) near surface for bath temperature of 200 °C

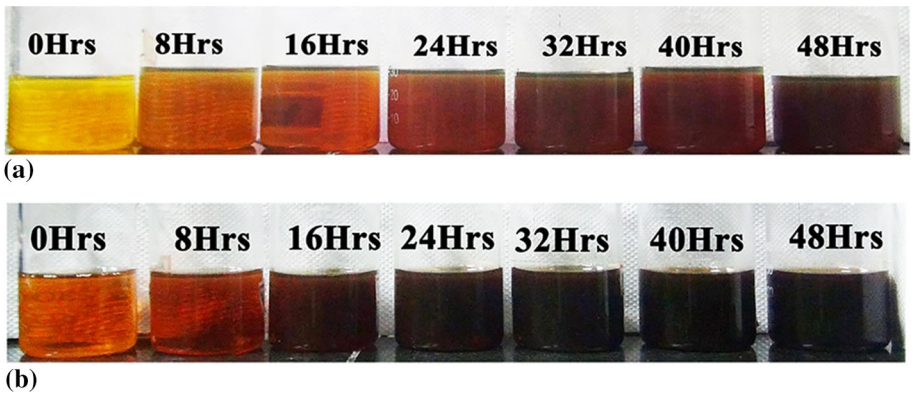

Fig. 13 Photographs of a) hot oil and b) neem oil oxidized in a hot air oven for varying periods of time

media maintained at 150 °C. The peak cooling rate was marginally higher in the case of oxidized neem oil, but the temperature corresponding to peak cooling rate was ~ 40 °C lower than non-oxidized neem oil. This lowering of peak cooling rate temperature was due to the occurrence of vapor blanket stage. Thus, the oxidation of neem oil resulted in a change from two-stage heat extraction mechanism (boiling and convective cooling stages) observed in non-oxidized neem oil to three-stage heat extraction mechanism (vapor blanket, boiling and convective cooling stages). Further, a decreased cooling rate was observed in the initial stage of quenching in oxidized neem oil. Subsequently, the cooling rate in oxidized neem oil was higher as compared to the non-oxidized neem oil. The increased cooling rate at the lower temperature would be helpful to suppress the bainitic transformation of austenite. However, the decreased cooling rate at the higher temperatures increases the propensity toward the transformation of austenite to pearlite, cementite and ferrite phases.

Oxidized neem oil has its advantages and limitations. On the one hand, the oxidation of oil prevents the transformation of

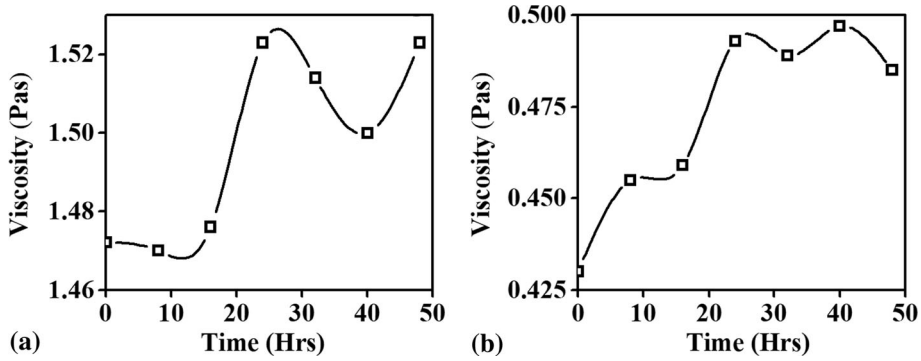

Fig. 14 Effect of oxidation on dynamic viscosity of (a) hot oil and (b) neem oil

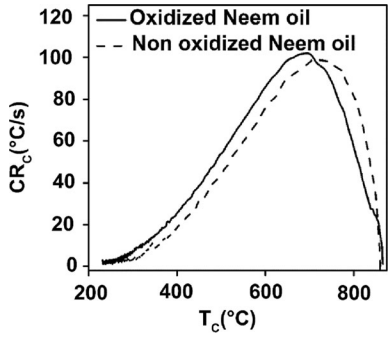

Fig. 15 Cooling rate v/s measured temperature curve at the geometric center of an Inconel probe quenched in oxidized and non-oxidized neem oil quench media maintained at 150 °C

bainite, whereas on the other it increases the propensity of transformation to pearlite. However, the effect of oxidation of neem oil on the overall quench heat extraction was observed to be minimal.

4. Conclusions

- Neem oil offered higher cooling rates and offered more uniform cooling of the Inconel probe as compared to hot oil.
- Quenching in neem oil resulted in higher hardness for AISI-52100 steel probes as compared to that quenched in hot oil.
- Pearlite in the microstructure of AISI-52100 steel probe quenched in hot oil maintained at 200 °C nullifies the purpose of hardening. Hot oils are therefore unsuitable quench media at this bath temperature.
- The effect of oxidation on the viscosity of neem oil is more pronounced compared to that of hot oil. The effect of oxidation on neem oil stabilized after 24 h of oxidation.
- Oxidation of neem oil resulted in the vapor blanket stage and decreased T_{max} and cooling rate at higher temperatures.
- Peak cooling rate and the cooling rate at lower temperatures were higher in the case of oxidized neem oil.
- Oxidation had a very limited effect on the cooling performance of hot neem oil quench medium and hence can be considered as an effective replacement for hot oil.

References

1. E.C. de Souza, M.R. Fernandes, S.C.M. Augustinho, L.C.F. Canale, and G.E. Totten, Comparison of Structure and Quenching Performance of Vegetable Oils, *J. ASTM Int.*, 2009, **6**(9), p 102188. https://doi.org/10.1520/jai102188
2. G. Ramesh and K.N. Prabhu, Wetting and Cooling Performance of Mineral Oils for Quench Heat Treatment of Steels, *ISIJ Int.*, 2014, **54**(6), p 1426–1435. https://doi.org/10.2355/isijinternational.54.1426
3. D.S. MacKenzie, Advances in quenching, in *Proceedings of the 22nd Heat Treating Society Conference and the 2nd International Surface Engineering Congress*, 2003 (Stage C), p. 228–239, https://doi.org/https://www.houghtonintl.com/sites/default/files/resources/article_-_advances_in_quenching.pdf
4. F. Salawa, R. Napierala, and C. Suarez, "Best Practices for the Application of Quenching Oils," n.d
5. E. Rowland and D.S. MacKenzie, "Proper Care of Quench Oil Leading to Consistent Part Quality," *Thermal Processing in Motion*, ASM International, 2018, p 98–105
6. G. Graham and D.S. Mackenzie, Understanding the Quenchant Report, 2018
7. N.J. Fox and G.W. Stachowiak, Vegetable Oil-Based Lubricants—A Review of Oxidation, *Tribol. Int.*, 2007, **40**(7), p 1035–1046
8. L.C.F. Canale, M.R. Fernandes, S.C.M. Agustinho, G.E. Totten, and A.F. Farah, Oxidation of Vegetable Oils and Its Impact on Quenching Performance, *Int. J. Mater. Prod. Technol.*, 2005, **24**(1/2/3/4), p 101. https://doi.org/10.1504/ijmpt.2005.007943
9. G.E. Totten, H.M. Tensi, and K. Lainer, Performance of Vegetable Oils as a Cooling Medium in Comparison to a Standard Mineral Oil, *J. Mater. Eng. Perform.*, 1999, **8**(4), p 409–416
10. K.M. Pranesh Rao and K.N. Prabhu, Assessment of Wetting Kinematics and Cooling Performance of Select Vegetable Oils and Mineral-Vegetable Oil Blend Quench Media, *Mater. Sci. Forum*, 2015, **830–831**, p 160–163. https://doi.org/10.4028/www.scientific.net/MSF.830-831.160
11. S.W. Dean, K.N. Prabhu, and P. Fernandes, Heat Transfer During Quenching and Assessment of Quench Severity—A Review, *J. ASTM Int.*, 2009, **6**(1), p 101784. https://doi.org/10.1520/jai101784
12. U.V. Nayak and K.N. Prabhu, Effect of Section Thickness on Heat Transfer during Quenching in Vegetable Oils, *Mater. Perform. Charact.*, 2018, **7**(1), p 20180084. https://doi.org/10.1520/mpc20180084
13. S.B. Hassan, J.B. Agboola, V.S. Aigbodion, and E.J. Williams, Hardening Characteristics of Plain Carbon Steel and Ductile Cast Iron Using Neem Oil as Quenchant, *J. Miner. Mater. Charact. Eng.*, 2011, **10**(2), p 161–172
14. H.K. Kim and S.I. Oh, Evaluation of Heat Transfer Coefficient during Heat Treatment by Inverse Analysis, *J. Mater. Process. Technol.*, 2001, **112**(2), p 157–165. https://doi.org/10.1016/S0924-0136(00)00877-3

15. Z. Nie, G. Wang, Y. Lin, and Y.K. Rong, Precision Measurement and Modeling of Quenching- Tempering Distortion in Low-Alloy Steel Components with Internal Threads, *J. Mater. Eng. Perform.*, 2015, **24**(12), p 4878–4889
16. K.M. Pranesh Rao and K.N. Prabhu, Effect of Bath Temperature on Cooling Performance of Molten Eutectic $NaNO_3$-KNO_3 Quench Medium for Martempering of Steels, *Metall. Mater. Trans. A*, 2017, **48**(10), p 4895–4904. https://doi.org/10.1007/s11661-017-4267-7
17. G. Ramesh and K.N. Prabhu, Assessment of Axial and Radial Heat Transfer during Immersion Quenching of Inconel 600 Probe, *Exp. Therm. Fluid Sci.*, 2014, **54**, p 158–170. https://doi.org/10.1016/j.expthermflusci.2014.01.016
18. S.R. Elmi Hosseini, A. Zabett, and Z. Li, Cooling Curve Analysis of Heat Treating Oils and Correlation with Hardness and Microstructure of a Low Carbon Steel, *Mater. Perform. Charact.*, 2015, **3**(4), p 20130067. https://doi.org/10.1520/mpc20130067